PAPER

Check for updates

Amphiphilic polymer-encapsulated Au nanoclusters with enhanced emission and stability for highly selective detection of hypochlorous acid†

Yiling Li, Shuxiao Yi, Zhongli Lei and Yan Xiao ID *

It is of vital importance to develop probes to monitor hypochlorous acid (HClO) in biological systems as HClO is associated with many important physiological and pathological processes. Metal nanoclusters (NCs) are promising luminescent nanomaterials for highly reactive oxygen species (hROS) detection on the basis of their strong reaction ability with hROS. However, metal NCs typically can respond to most common hROS and are susceptible to etching by biothiols, hindering their application in the construction of effective HClO probes. Herein, we proposed a strategy to develop a nanoprobe based on Au NCs for highly sensitive and selective detection of HClO. We synthesized luminescent benzyl mercaptan-stabilized Au NCs and encapsulated them with an amphiphilic polymer (DSPE-PEG). After encapsulation, an obvious emission enhancement and good resistance to the etching by biothiols for Au NCs were achieved. More importantly, the DSPE-PEG encapsulated Au NCs can be used as a nanoprobe for detection of HClO with good performance. The luminescence of the Au NCs was effectively and selectively quenched by HClO. A good linear relationship with the concentration of HClO in the range of 5–35 μM and a limit of detection (LOD) of 1.4 μM were obtained. Additionally, this nanoprobe was successfully used for bioimaging and monitoring of HClO changes in live cells, suggesting the application potential of the as-prepared amphiphilic polymer-encapsulated Au NCs for further HClO-related biomedical research.

Introduction

Hypochlorous acid (HClO) is a kind of highly reactive oxygen species (hROS) widely present in living organism. It is generated from the reaction of hydrogen peroxide and chloride ions under the catalysis of myeloperoxidase.[1] HClO plays an important role in many important physiological and pathological processes, such as the body's autoimmune response against pathogen invasion. The normal physiological concentration of HClO is generally 5–25 μM,[2] but when inflammation occurs, cells can produce in excess of 100 μM HClO.[3] Excessive production of HClO *in vivo* will oxidize biological molecules and cause tissue damage, and even lead to many diseases, including arthritogensis, cardiovascular diseases, and cancer.[4–6] For these reasons, identifying HClO inside biological cells with precise detection is of great significance for biological research and clinical diagnosis. However, selective detection of HClO at low concentrations *in vivo* becomes particularly difficult due to its high reaction activity, the presence of antioxidants such as glutathione and interference from other active substances.[7] Therefore the development of analytical methods that can detect HClO with high efficiency and selectivity *in vivo* is still worth exploring.

In recent years, fluorescent analytical methods have been widely used in the detection of HClO due to their simple operation, rapid-response and real-time monitoring capabilities, showing tremendous potential in medical diagnosis and research.[8–11] Currently, some fluorescent probes for the detection of HClO have been developed and most of them are organic molecular probes.[12–14] Although these organic fluorescent probes have made great progresses in HClO detection, there are still some defects, which limit their applications, such as complex synthesis process, poor photostability and water-solubility, spontaneous autoxidation and toxicity concerns. Therefore, there is still a great demand to design fluorescent probes with good performance for the detection of HClO.

Metal nanoclusters (NCs) have drawn broad interests in the construction of luminescence probes for bioanalysis in terms of their facile synthesis, ultra-small size, large Stokes shift, good

Collaborative Innovation Center for Advanced Organic Chemical Materials Co-constructed by the Province and Ministry, Ministry of Education Key Laboratory for the Synthesis and Application of Organic Functional Molecules, College of Chemistry and Chemical Engineering, Hubei University, Wuhan 430062, China. E-mail: xiaoyan@hubu.edu.cn

biocompatibility and photobleaching resistance.[15–17] In view of their unique composition and ultra-small size, metal NCs are easy to be oxidized by surrounding strong oxidizing substances, leading to the luminescence quenching.[18,19] Therefore, it is an attractive alternative to develop luminescent nanoprobes for the sensitive and effective detection of hROS based on metal NCs. Recent years have witnessed the development in this aspect. Several luminescent nanoprobes based on the oxidation of Au NCs by hROS have been designed and developed. For examples, Chen *et al.* constructed a dual-emission nanoprobe for *in situ* ratiometric detection of hROS by decorating dye encapsulated silica nanoparticles with glutathione (GSH) stabilized-Au NCs.[20] Jiang and co-workers decorated GSH-Au NCs with the cell-penetrating oligoarginine peptide to improve the cellular uptake of Au NCs for intracellular hROS detection *via* fluorescence quenching.[21] Cao *et al.* prepared a nanoprobe through encapsulating GSH-Au NCs in nanoscale metal–organic frameworks for sensitive monitoring and bioimaging hROS in living cells.[22] However, these methods cannot distinguish different hROS to achieve the highly selective detection of different hROS. Moreover, these water-soluble nanoprobes tend to be attacked by biothiols (*e.g.* GSH, Cys) which are ubiquitous in biological systems since sulfhydryl group has a strong affinity for noble metals.[23] This will lead to instability and inaccuracy in analysis. These drawbacks seriously hamper their utility for practical analysis applications and selective HClO detection. There are crucial needs in the area of metal NCs based hROS detection for improving the selectivity for hROS and reinforcing the stability of metal NCs in biological systems. It is highly challenging but rewarding to devote efforts to improve performance of metal NCs and use them for selective detection of HClO.

In this work, we presented an effective strategy to circumvent these barriers and developed a luminescent nanoprobe based on Au NCs for HClO detection with high selectivity and stability. We synthesized luminescent benzyl mercaptan-stabilized Au NCs (BM-Au NCs) and encapsulated them with an amphiphilic polymer (DSPE-PEG).[24] The encapsulation of hydrophobic BM-Au NCs with amphiphilic DSPE-PEG validly improved the luminescence and stability of Au NCs. The as-synthesized DSPE-PEG encapsulated Au NCs (DSPE-PEG-Au NCs) not only exhibit an enhanced emission but also excellent stability in physiological environment including good resistance to the etching by biothiols. More importantly, the encapsulation of Au NCs endowed them with the ability to selectively detect HClO over other hROS. Among hROS, only HClO can oxidize the Au NCs in the hydrophobic core of micelles and cause the quenching of luminescence. This may be due to the weak oxidants cannot oxidize Au NCs, while other hROS generated in aqueous solution with very short life are difficult to diffuse across the surface polymer coatings and reach to Au NCs.[25] Therefore, the luminescence quenching of Au NCs by HClO-induced oxidation can be used for the sensitive and selective detection of HClO. The DSPE-PEG-Au NCs are capable of being a nanoprobe for imaging of the changes in intracellular HClO levels. This work provides an effective strategy to design a nanoprobe based on Au NCs for HClO detection with high selectivity and good anti-

interference ability. Benefiting from its outstanding performance, the as-constructed analytical method may have great potential for further biomedical application.

Experimental

Materials and instruments

HAuCl$_4$·4H$_2$O was purchased from Chemical Reagent Co., Ltd (Shanghai, China). NaBH$_4$ was purchased from Lingfeng Chemical Reagent Co., Ltd (Shanghai, China). Tetraoctylammonium bromide (TOAB, 98%), DSPE-PEG$_{5000}$ (95%), benzyl mercaptan (PhCH$_2$SH, 98%) and 2-phenylethanethiol (PhC$_2$H$_4$SH, 97%) were purchased from Aladdin Ltd (Shanghai, China). Sodium hypochlorite (NaClO) was bought from Bailingwei Technology Co., Ltd (Beijing, China). Bovine serum albumin (BSA) was bought from Yuanye Biological Technology Co., Ltd (Shanghai, China). Tetrahydrofuran (THF, 99.0%), hydrogen peroxide (H$_2$O$_2$, 30%), methanol (CH$_3$OH, 99.5%), dichloromethane (CH$_2$Cl$_2$, 99.0%) and the rest of reagents were bought from Sinopharm Chemical Reagent Co., Ltd (Shanghai, China). All mentioned reagents were of analytical grade and commercialized without further purification. The glassware used in the experiment was soaked in aqua regia beforehand. The aqueous solutions used in the experiments were prepared using ultrapure water (Millipore Milli-Q, 18.25 MΩ cm).

Fluorescence spectra were recorded on a RF-5301 fluorophotometer (Shimadzu, Japan) with slit width at 10 nm for both excitation and emission. UV-vis spectroscopic studies were carried out on a UH 4150 UV-vis spectrophotometer (Hitach, Japan). Dynamic light scattering (DLS) measurements were performed on a Zetasizer Nano from Malvern Instruments. Transmission electron microscopy (TEM, JEM-2010, 200 kV) was used to determine the size and morphology of nanomaterials. FT-IR spectra were conducted on a NEXUS640 infrared spectrometer system (NICOLET iS10, USA) with the KBr pellet technique. X-ray photoelectron spectroscopy (XPS) spectra were obtained from an ESCALAB 250Xi (Thermo scientific, USA).

Synthesis of benzyl mercaptan-stabilized Au NCs (BM-Au NCs)

In brief,[26] TOAB (0.12 mmol, 0.065 g) and HAuCl$_4$ (0.1 mmol) were mixed in THF and stirred for 15 min. Then, PhC$_2$H$_4$SH (0.5 mmol, 65 μL) was added to the mixture. After stirring for 2 h, NaBH$_4$ aqueous solution (1 mmol, 0.0375 g) was quickly added into the above mixture and the solution was vigorous stirred for 5 min. Subsequently, the stirring speed was slowed down and the reaction was allowed to further proceed for 10 h. After removing the insoluble byproduct by centrifugation, the reaction mixture was evaporated and the residue was collected and washed with methanol three times. Next,[27] 10 mg of washed solid was dissolved in 1 mL of dichloromethane. Then, 0.25 mL of PhCH$_2$SH was added to the solution followed by vigorous stirring for 18 h at room temperature. After synthesis, a large amount of methanol was added to terminate the reaction and precipitate the as-synthesized Au NCs. The precipitate was collected and washed with methanol three times.

Synthesis of DSPE-PEG encapsulated Au NCs

The DSPE-PEG encapsulated Au NCs (DSPE-PEG-Au NCs) were prepared using a solvent evaporation method.[28] First, 1 mg of DSPE-PEG$_{5000}$ and 1 mg of BM-Au NCs were dissolved in 2.5 mL THF and sonicated for 5 min. Then, the prepared mixed solution was slowly added dropwise to water (5 mL) and treated with ultrasound until a homogenous mixture was obtained. Subsequently, the low-boiling THF in the mixture was removed under reduced pressure at 40 °C to form a micelle solution. Finally, the DSPE-PEG encapsulated benzyl mercaptan-stabilized Au NCs were obtained and stored at 4 °C for the further use.

Fluorescence responses to hypochlorous acid

The DSPE-PEG-Au NCs were first diluted with a PBS (10 mM, pH = 7.4) buffer solution to a final concentration of 0.13 mg mL^{-1}. Then, various concentrations (0–150 μM) of freshly prepared sodium hypochlorite (NaClO) solutions were added into DSPE-PEG-Au NCs and incubated for 1 min at 37 °C. The HClO concentrations were determined by UV absorbance at 292 nm (ε = 350 M^{-1} cm^{-1}). Subsequently, the fluorescence emission spectra of Au NCs were recorded with an excitation wavelength of 400 nm.

In order to evaluate the selectivity of the DSPE-PEG-Au NCs toward hypochlorous acid, some other substances, including common ROS, amino acids, metal ions, and biomolecules were added in place of HClO with the same experimental conditions and procedures. Hydroxyl radical (·OH) was generated by Fenton reaction (Fe^{2+} + H$_2$O$_2$ → Fe^{3+} + ·OH + OH$^-$) by mixing FeSO$_4$·7H$_2$O with H$_2$O$_2$ at a molar ratio of 1 : 10 at 37 °C. ONOO$^-$ was obtained by the reaction between NaNO$_2$ and H$_2$O$_2$ at a molar ratio of 1 : 5.[29–31]

Cellular imaging

For cellular imaging experiments, HeLa cells were first plated on cell culture dishes and allowed to adhere for 24 h. To detect exogenous HClO, HeLa cells were then incubated in culture medium containing DSPE-PEG-Au NCs (final concentration: 300 μg mL^{-1}) at 37 °C for 6 h. Next, the cells were washed with PBS to remove extracellular excess DSPE-PEG-Au NCs nanoprobes. After that, the cells were treated with different concentrations of HClO in DMEM for 30 min. For controls, incubation was continued for 30 min with DMEM without HClO. Then, the cell fluorescence imaging experiments were carried out.

For the detection of endogenous HClO, under 37 °C incubation conditions, HeLa cells were treated with LPS (1 μg mL^{-1}) for 12 h, PMA (10 nM) for 30 min, and finally incubated with DSPE-PEG-Au NCs for 6 h. After washed three times, the cells were subjected to cell imaging. Control sections were incubated with UA (250 nM) and DMSO (0.5%) for 15 minutes followed by the same treatment with LPS, PMA, and the probe for an additional 6 h. All fluorescence images were acquired on confocal fluorescence microscopy analysis. Excitation: 405 nm. Emission collection: 600–700 nm.

Results and discussion

Design principle

Effective methods for detection of HClO are extremely necessary as HClO is a kind of hROS widely present in living organism and plays crucial roles in many physiological processes. Since metal NCs are liable to be oxidized by hROS,[32] they are promising luminescent nanomaterials to construct nanoprobes for hROS detection. However, metal NCs typically can react with most of common hROS and are susceptible to etch by biothiols, limiting their application for construction of HClO probes.[33] To realize the selective and stable detection of HClO based on metal NCs, we adopted a strategy of encapsulating hydrophobic Au NCs with an amphiphilic polymer. We first synthesized benzyl mercaptan-stabilized Au NCs (BM-Au NCs) with aggregation-induced emission (AIE) feature. Using amphiphilic polymer DSPE-PEG as a nanocarrier, the hydrophobic BM-Au NCs can be encapsulated into DSPE-PEG by the method of solvent volatilization. After encapsulation, the BM-Au NCs formed tight aggregates and thereby the luminescence of Au NCs was significantly improved for analysis application.[34] In the meantime, the as-prepared DSPE-PEG encapsulated Au NCs (DSPE-PEG-Au NCs) exhibited satisfactory stabilities under physiological conditions. In particular, the encapsulation with amphiphilic polymer can well isolate hydrophobic Au NCs with water-soluble biothiols and make DSPE-PEG-Au NCs are resistant to the etching by biothiols that is often lacking for metal NCs. Leveraging on the encapsulation with polymer, the DSPE-PEG-Au NCs can be used as a nanoprobe for sensitive and selective detection of HClO in living cells. Among common hROS, only HClO can enter the polymer interior to react with Au NCs, resulting in luminescence quenching, as illustrated in Scheme 1. This may be due to the strong oxidizing power of HClO, while other very short-lived hROS generated in aqueous solution are difficult to diffuse in the polymer surface coating and reach the Au NCS.[35,36] The luminescence change of Au NCs caused by HClO is capable of detection of intercellular HClO level.

Synthesis and characterization of BM-Au NCs and DSPE-PEG-Au NCs

In this work, we used water-soluble HAuCl$_4$ as the precursor to prepare the luminescent benzyl mercaptan-stabilized Au NCs. The HAuCl$_4$ were first transferred to the organic phase by a phase transfer agent and followed by reduction with NaBH$_4$ in
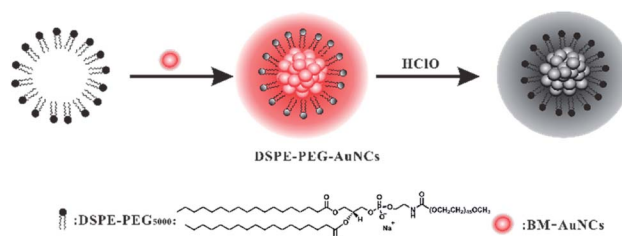
Scheme 1 Schematic diagram of the preparation of DSPE-PEG encapsulated Au NCs and their application in the detection of HClO.

the presence of phenylethanethiol. Then, benzyl mercaptan was introduced to etch the reduction products to obtain the final luminescent BM-Au NCs (Fig. S1†). The as-prepared nano-materials were well characterized by UV-vis absorption and fluorescence spectroscopy, X-ray photoelectron spectroscopy (XPS) and transmission electron microscope (TEM). We investigated the optical properties of the BM-Au NCs by UV-vis absorption and fluorescence spectroscopy. As shown in Fig. 1A, the BM-Au NCs exhibited weak absorption around 500 nm and a luminescence emission peak centered at 650 nm. The solid Au NCs were orange under visible light, and emitted strong red photoluminescence (PL) under the irradiation of UV-light at 365 nm (Fig. 1A, inset). Next, we ascertained the reduction of Au(III) and the surface interaction between metal core and ligands by XPS analysis (Fig. S2†). The XPS data for Au species showed two well distinguished peaks at 83.9 eV and 87.5 eV, corresponding to Au $4f_{7/2}$ and Au $4f_{5/2}$, respectively.[37] The Au $4f_{7/2}$ peak was centered at 83.9 eV, between Au(I)-thiolate (86.0 eV) and bulk Au (83.8 eV),[38,39] confirming the reduction of Au(III) and the coexistence of Au(0) and Au(I) in the Au NCs. Additionally, the binding energy of S $2p_{3/2}$ located at 162.4 eV which are in a good agreement with the typical value of chemisorbed S species,[40] demonstrating the interaction of Au NCs with benzyl mercaptan through the Au–S bond.[41] The morphology and size of the BM-Au NCs were studied by TEM. As presented in Fig. 1B, the TEM image of BM-Au NCs indicated that the BM-Au NCs exhibited spherical shape with a diameter of 1.36 ± 0.66 nm. These results highly proved that we successfully prepared ultra-small BM-Au NCs.

To improve the PL performance and stability of Au NCs and obtain the ability for selective HClO detection, DSPE-PEG, a biocompatible and biodegradable amphiphilic polymer, was utilized to form micelle and encapsulate BM-Au NCs via a solvent evaporation method. First, the mixed BM-Au NCs and DSPE-PEG in tetrahydrofuran (THF) was slowly added dropwise to water and treated with ultrasound to obtain a homogenous mixture. With the gradually volatilizing of THF, the hydrophilic end of DSPE-PEG was self-assembled to form micelle in water. In this process, the hydrophobic BM-Au NCs reached the hydrophobic core of the micelle through hydrophobic interactions, thus obtaining DSPE-PEG encapsulated Au NCs (DSPE-PEG-Au NCs). For the characterization of the DSPE-PEG-Au NCs, we conducted TEM and Fourier transform infrared spectra (FT-IR) analysis. The TEM image of DSPE-PEG-Au NCs showed they were consisted of a core with densely packed ultra-small BM-Au NCs (Fig. 1C). The average size of core was about 62 ± 18 nm. FT-IR analysis was also used to demonstrate the formation of DSPE-PEG encapsulated Au NCs. In the FT-IR spectrum of DSPE-PEG-Au NCs, there was a broad and strong band at 3442 cm^{-1}, which was attributed to the stretching vibration of N–H (Fig. S3†). Additionally, the peak at 1599 cm^{-1} was ascribed to C=O stretching vibration. The present of these vibration absorptions of DSPE-PEG in the FT-IR spectrum of DSPE-PEG-Au NCs indicated BM-Au NCs had been successfully further modified with DSPE-PEG.

After confirming the successful synthesis of DSPE-PEG encapsulated Au NCs, we investigated the PL change of Au NCs. The as-formed aggregated Au NCs showed obvious brighter red emission when compared to dispersive BM-Au NCs (Fig. 1D), indicating that the BM-Au NCs possess aggregation-induced emission feature. A significant enhancement of the emission of Au NCs which is extremely important for their bioanalysis application can be achieved via this encapsulation.[42] Furthermore, we studied the stability of DSPE-PEG-Au NCs under different conditions. As displayed in Fig. 2A, the influence of pH of solution on the luminescence of DSPE-PEG-Au NCs was examined. The luminescence of DSPE-PEG-Au NCs was slightly enhanced with increasing of pH and strong
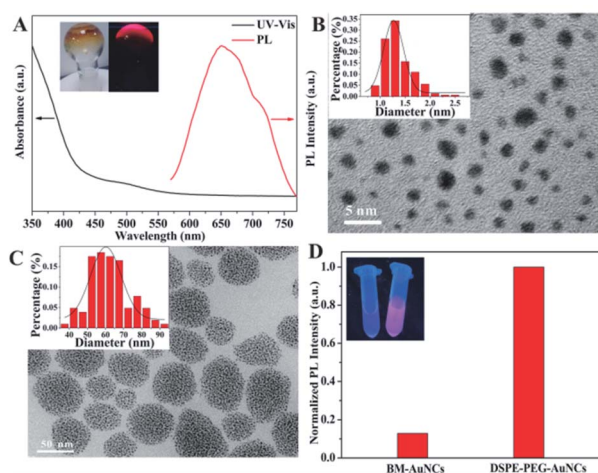
Fig. 1 (A) UV-vis absorption (black line) and PL (red line, λ_{ex} = 400 nm) spectra of BM-Au NCs. Insets: digital pictures of the BM-Au NCs under white (left) and UV (right) light. (B) TEM image of BM-Au NCs. Inset: size distribution histogram of BM-Au NCs. (C) TEM image of DSPE-PEG-Au NCs. Inset: size distribution histogram of DSPE-PEG-Au NCs. (D) The change of PL intensity of Au NCs after encapsulating with DSPE-PEG. Insets: digital pictures of BM-Au NCs (left) and DSPE-PEG-Au NCs (right) under UV excitation.
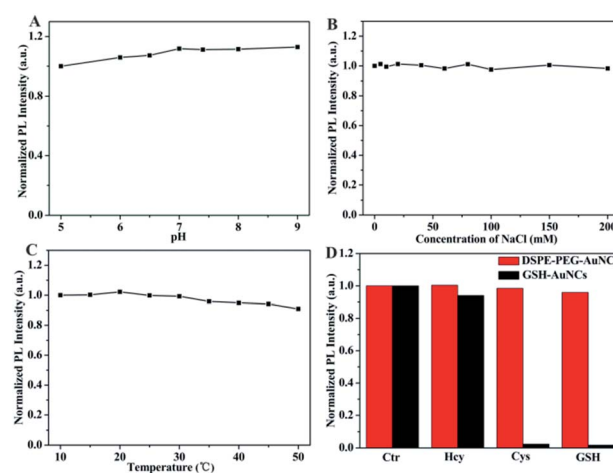
Fig. 2 Normalized PL intensity of DSPE-PEG-Au NCs at different pH values (A); in NaCl aqueous solution with different concentrations (B); at different temperatures (C); and in present of different biothiols (Hcy: 15 μM, Cys: 300 μM, GSH: 10 mM) (D).

emission was still observed in physiological buffer at pH 7.4. Besides, the DSPE-PEG-Au NCs exhibited excellent stability in high concentration salt solution. The emission intensity of DSPE-PEG-Au NCs in NaCl aqueous solutions nearly showed little changes with the concentrations of NaCl increasing from 0 to 0.2 M (Fig. 2B). Moreover, the effect of temperature on the luminescent stability of DSPE-PEG-Au NCs was also investigated from 10 to 50 °C. The data in Fig. 2C showed that the emission intensity of DSPE-PEG-Au NCs only dropped a little as the temperature increased, inferring a good temperature stability of DSPE-PEG-Au NCs. More importantly, the DSPE-PEG-Au NCs presented obvious anti-sulfhydryl etching ability. According to the previous studies, common biothiols thiols *in vivo* include Hcy (5–15 μM),[43] Cys (100–300 μM),[44] and GSH (1–10 mM).[45] Considering these, we investigated the luminescence stability of DSPE-PEG-Au NCs in presence of 15 μM Hcy, 300 μM Cys and 10 mM GSH, respectively. Compared with the GSH-Au NCs, biothiols have evident less effect on the luminescence of the DSPE-PEG-Au NCs (Fig. 2D). These experimental studies illustrated that the as-synthesized DSPE-PEG-Au NCs possess strong luminescence, outstanding stability and attractive prospects for practical application in biological systems.

Determination of hypochlorous acid

Such a high stability and enhanced emission of DSPE-PEG-Au NCs motivated us to explore its promising application in HClO detection. Inspiringly, we found the fluorescence of DSPE-PEG-Au NCs was remarkably and selectively quenched in the presence of HClO (Fig. 3A). To verify the mechanism of luminescence quenching, we conducted a series of characterization and control experiments. Firstly, we investigated the hydrodynamic sizes of the DSPE-PEG-Au NCs after the addition of HClO by dynamic light scattering (DLS) measurement. Various amount of HClO were added into the DSPE-PEG-Au NCs to observe the change of nanoparticles sizes. The results showed the hydrodynamic diameters of DSPE-PEG-Au NCs remained

stable with the introduction of HClO, suggesting HClO did not destroy the aggregates of Au NCs (Fig. 3B). In addition, the FT-IR spectrum of DSPE-PEG-AuNCs was highly similar to those of HClO quenched samples, indicating that the polymer covering the Au NCs had not been damaged (Fig. 3C). At the same time, the zeta-potential of the DSPE-PEG-Au NCs had not changed significantly in the presence of HClO (Fig. 3D), which illustrated that the surface states of DSPE-PEG-Au NCs unchanged. Therefore, the PL quenching may not result from the weakening of the AIE of Au NCs by the breakdown of the encapsulation but the direct reaction between HClO and Au NCs. To further gain insights into the mechanism of HClO-induced luminescence quenching, we studied the luminescence lifetime change of DSPE-PEG-Au NCs after the addition of HClO (Fig. S4†). It was found that there was no obvious change in the luminescence lifetime when HClO was added to DSPE-PEG-Au NCs, which ruled out the dynamic quenching mechanisms. Taking these into consideration, we speculated the quenching was caused by oxidation of Au NCs since HClO has strong oxidizing ability. In order to prove this assumption, we used XPS analysis to examine the effect of HClO on the oxidation state of Au NCs. As displayed in Fig. S5,† the Au4f$_{7/2}$ peaks in DSPE-PEG-Au NCs could be deconvoluted into 83.5 and 84.1 eV, corresponding to Au(0) and Au(ɪ), respectively. The percent of Au(ɪ) was about 35.7%. When the DSPE-PEG-Au NCs were exposed to HClO, the percent of Au(ɪ) was increased to be 48.4%. Additionally, we studied the amperometric time curves of DSPE-PEG-Au NCs upon successive injections of HClO. The response current continuously decreased with the addition of HClO under constant potentials, confirming the occurring of redox reaction between DSPE-PEG-Au NCs and HClO (Fig. S6†).[46–48] The above evidence verified the oxidation of Au NCs is the reason for the HClO-induced fluorescence quenching of DSPE-PEG-Au NCs.

The detection of HClO can be carried out by this PL quenching. Before utilizing the DSPE-PEG-Au NCs for the HClO detection, several reaction conditions were first optimized to obtain good analysis performances. Fig. S7A† illustrated the influence of pH on the HClO-induced PL quenching of Au NCs. The degree of fluorescence quenching was slightly decreased with the pH of solution increased from 5–9. This phenomenon was due to the pH-dependent distribution of HClO. With the increasing of pH, the present of HClO in the solution was decreased, leading to the weakening of quenching effect.[36,49] Considering the pH of the physiological environment, pH 7.4 was chosen for subsequent HClO detection. As depicted in Fig. S7B,† the luminescence intensity of DSPE-PEG-Au NCs decreased significantly with the reaction time increased from 0 to 50 s and then remained constant, indicating that DSPE-PEG-Au NCs can act as a "fast response" luminescent nanoprobe for HClO detection. Hence, in the following experiments, we selected pH of 7.4 and incubation time of 1 min for HClO detection.

Under the optimal condition, different concentrations of HClO were added into the DSPE-PEG-Au NCs nanoprobes solution. The luminescence intensity of the DSPE-PEG-Au NCs decreased with the HClO concentration changed from 5 to 80 μM (Fig. 4A and B). When the concentration of HClO reached at
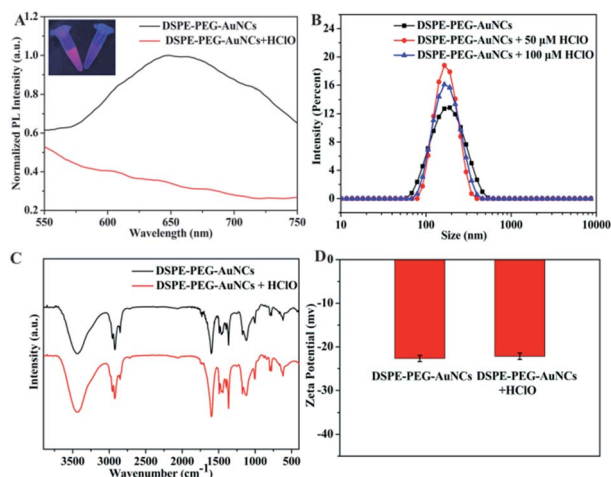

Fig. 3 PL intensity spectra (A), dynamic light scattering (B), FT-IR spectra (C) and zeta potentials (D) of the DSPE–PEG–Au NCs before and after the addition of HClO.
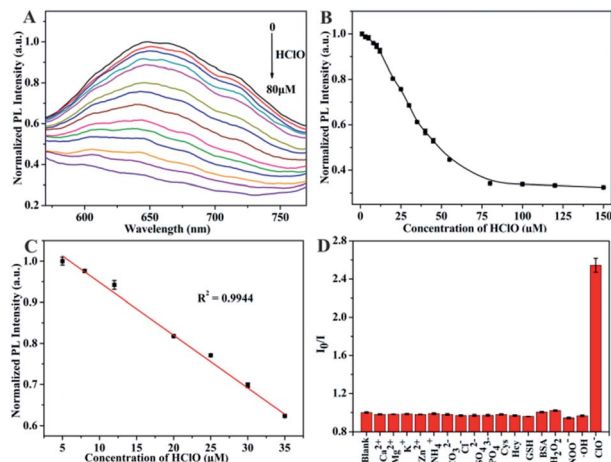
Fig. 4 (A) PL spectra of DSPE–PEG–Au NCs (0.13 mg mL^{-1}) in the presence of different concentrations of HClO (0–80 μM). (B) The PL intensity of DSPE–PEG–Au NCs in response to varying concentrations of HClO. (C) The linear relationship between the PL intensity of DSPE–PEG–Au NCs and the concentration of HClO. (D) The relative fluorescence intensity of DSPE–PEG–Au NCs in the presence of different substances (I and I_0 represents the fluorescence intensity of DSPE–PEG–Au NCs in the presence and absence of the detection substances, respectively). The concentration of all tested species is 100 μM. λ_{ex} = 400 nm.

Bioimaging of hypochlorous acid in living cells

With the features of high sensitivity and selectivity, DSPE–PEG–Au NCs as a nanoprobe for HClO detection may achieve good application in living cells. We then sought to test this hypothesis. Before imaging of HClO in living cells, we assessed the biocompatibility of the DSPE–PEG–Au NCs nanoprobe. The cytotoxicity of the nanoprobe was firstly evaluated using the standard MTT assay. It was observed that the cellular viabilities were estimated to be greater than 85% in the presence of the nanoprobes with concentration from 0–300 μg mL^{-1} (Fig. S8†). The results indicated the nanoprobe showed low cytotoxicity in HeLa cells, suggesting their excellent biocompatibility. To demonstrate the potential biological applications of the DSPE–PEG–Au NCs, the imaging of exogenous and endogenous HClO in living cells was carried out using DSPE–PEG–Au NCs as a nanoprobe. After the HeLa cells were incubated with the nanoprobe, a distinguishable fluorescence signal in the red channel was observed (Fig. 5), which confirmed that the DSPE–PEG–Au NCs had a good cell penetration capacity. For exogenous HClO detection, after incubated with the nanoprobe, the cells were further treated with different concentrations of HClO for 30 min at 37 °C. With the increase of HClO concentration, the red luminescence of DSPE–PEG–Au NCs in HeLa cells was dramatically weakened (Fig. 5). For endogenous HClO detection, as shown in Fig. S9,† HeLa cells only incubated with the nanoprobe showed strong red fluorescence, while the cells pretreated with lipopolysaccharide (LPS) and phorbol myristate acetate (PMA) showed weak red fluorescence. This is because hypochlorous acid produced by costimulation of the cells with LPS and PMA caused the fluorescence quenching of the nanoprobe.[52] In addition, red fluorescence recovery was observed upon cells were treated with dimethyl sulfoxide (DMSO) and uric acid (UA) after LPS/PMA stimulation. The recovery of fluorescence is attributed to the effective removal of
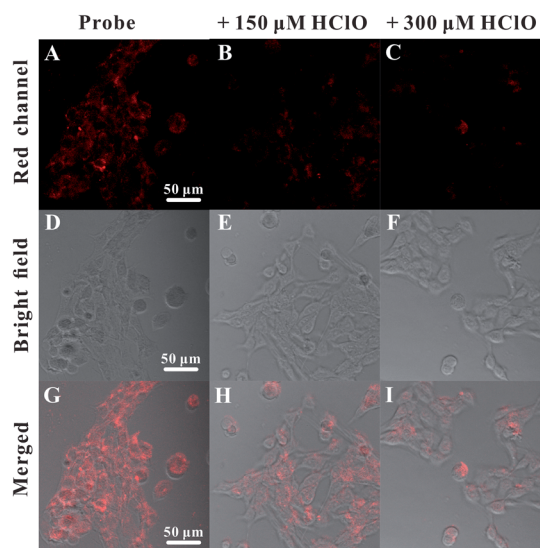
80 μM, the luminescence of Au NCs was almost completely quenched. A good linear relationship between the fluorescence intensity of DSPE–PEG–Au NCs and HClO concentration over the range of 5–35 μM was obtained (Fig. 4C). The linear equation could be represented by $Y = 1.076 - 0.012X$ with the correlation coefficient of $R^2 = 0.9944$. The limit of detection (LOD) was calculated to be 1.4 μM according to the equation LOD = 3σ/slope, where σ is the standard deviation for the fluorescent intensity of DSPE–PEG–Au NCs in the absence of HClO. These results declared that DSPE–PEG encapsulated Au NCs can realize highly effective detection of HClO *via* quenching the luminescence of DSPE–PEG–Au NCs.

Selectivity is an important evaluation parameter for the performance of luminescent nanoprobes.[50] We then assessed the selectivity of our DSPE–PEG–Au NCs nanoprobe towards HClO. We tested the response of our nanoprobe to the common biologically important ROS including H$_2$O$_2$, ONOO$^-$ and ·OH and found that only HClO rapidly quenched the luminescence of DSPE–PEG–Au NCs, whereas other ROS showed no obvious quenching effects (Fig. 4D). The high selectivity of DSPE–PEG–Au NCs for HClO over other ROS may be attributed to the effective HClO diffusion into the hydrophobic cavity through the polymer shell of nanomaterials. As a result, the oxidation of Au NCs by HClO led to fluorescence quenching.[35,51] To further evaluate the selectivity of the nanoprobe, the PL of DSPE–PEG–Au NCs in the present of various biologically relevant ions and molecules, such as metal ions and amino acids were also investigated. The data were showed in Fig. 4D. Based on the results of selectivity experiments, the tested biomolecules or ions had neglectable influence on the luminescence of DSPE–PEG–Au NCs, indicating a high selectivity of the nanoprobe for HClO.

Fig. 5 Fluorescence images of HeLa cells incubated with the nanoprobes and different amounts of exogenous HClO ((A, D and G) 0, (B, E and H) 150 and (C, F and I) 300 μM). Scale bar was 50 μm.

intracellular HClO by DMSO and UA.[53] These results indicated that the DSPE-PEG-Au NCs are capable of acting as a luminescent nanoprobe for monitoring the changes of intracellular HClO concentration.

Conclusions

In summary, we have successfully developed a sensitive and selective luminescent nanoprobe for the detection of HClO based on Au NCs. We synthesized luminescent benzyl mercaptan-stabilized Au NCs and encapsulated them with an amphiphilic polymer. This encapsulation effectively improved the luminescence and stability of Au NCs and endowed them with ability to selectively detect HClO. The emission of Au NCs was greatly enhanced via the encapsulation triggered AIE of Au NCs. Additionally, the as-prepared DSPE-PEG encapsulated Au NCs exhibit excellent stabilities, including a good resistance to etching by biothiols that is typically lacking for metal NCs. HClO with strong oxidizing capacity can diffused across the layer of surface polymer coatings and react with Au NCs to quench the luminescence of DSPE-PEG Au NCs rapidly. This phenomenon was successfully used for detection of HClO and bioimaging of changes in the cellular HClO level in living cells. This work provides an effective method to develop nanoprobe based on metal NCs for HClO detection with good performance. The as-prepared amphiphilic polymer-encapsulated Au NCs with good luminescence and stability may have great potential for further HClO-related biomedical studies.

Conflicts of interest

There are no conflicts to declare.

Acknowledgements

References

1 C. C. Winterbourn and A. J. Kettle, *Free Radical Bio. Med.*, 2000, **29**, 403–409.
2 M. C. Mancini, B. A. Kairdolf, A. M. Smith and S. Nie, *J. Am. Chem. Soc.*, 2008, **130**, 10836–10837.
3 B. M. Babior, *Am. J. Med.*, 2000, **109**, 33–44.
4 J. K. Andersen, *Nat. Med.*, 2004, **5**, S18–S25.
5 S. Baldus, C. Heeschen, T. Meinertz, A. M. Zeiher, J. P. Eiserich, T. Münzel, M. L. Simoons and C. W. Hamm, *Circulation*, 2003, **108**, 1440–1445.
6 J. Perez-Vilar and R. C. Boucher, *Free Radic. Biol. Med.*, 2004, **37**, 1564–1577.
7 S. Parvez, M. J. C. Long, J. R. Poganik and Y. Aye, *Chem. Rev.*, 2018, **118**, 8798–8888.
8 K. P. Carter, A. M. Young and A. E. Palmer, *Chem. Rev.*, 2014, **114**, 4564–4601.

9 X. Q. Chen, X. Z. Tian, I. Shin and J. Yoon, *Chem. Soc. Rev.*, 2011, **40**, 4783–4804.
10 J. Y. Han and K. Burgess, *Chem. Rev.*, 2010, **110**, 2709–2728.
11 Y. Zhou, J. F. Zhang and J. Yoon, *Chem. Rev.*, 2014, **114**, 5511–5571.
12 J. B. Claver, M. C. V. Mirón and L. F. Capitán-Vallvey, *Anal. Chim. Acta*, 2002, **522**, 267–273.
13 O. Ordeig, R. Mas, J. Gonzalo, F. J. d. Campo, F. X. M. Pascual and C. d. Haro, *Electroanalysis*, 2005, **17**, 1641–1648.
14 N. O. Soto, B. Horstkotte, J. G. March, P. L. L. d. Alba, L. L. Martínez and V. C. Martín, *Anal. Chim. Acta*, 2008, **611**, 182–186.
15 M. J. Abrams and B. A. Murrer, *Science*, 1993, **261**, 725–730.
16 L. Y. Chen, C. W. Wang, Z. Q. Yuan and H. T. Chang, *Anal. Chem.*, 2015, **87**, 216–229.
17 T. Wang, Y. Zhang, Q. C. Liu, W. Cheng, X. R. Wang, L. J. Pan, B. X. Xu and H. X. Xu, *Adv. Funct. Mater.*, 2018, **28**, 1705551.
18 C. X. Niu, Q. L. Liu, Z. H. Shang, L. Zhao and J. Ouyang, *Nanoscale*, 2015, **7**, 8457–8465.
19 X. Y. Mu, L. Qi, P. Dong, J. Qiao, J. Hou, Z. X. Nie and H. M. Ma, *Biosens. Bioelectron.*, 2013, **49**, 249–255.
20 T. T. Chen, Y. H. Hu, Y. Cen, X. Chu and Y. Lu, *J. Am. Chem. Soc.*, 2013, **135**, 11595–11602.
21 Y. Z. Y. Xie, Y. L. Xianyu, N. X. Wang, Z. Y. Yan, Y. Liu, K. Zhu, N. S. Hatzakis and X. Y. Jiang, *Adv. Funct. Mater.*, 2018, **28**, 1702026.
22 X. Y. Cao, S. S. Cheng, Y. You, S. M. Zhang and Y. Z. Xian, *Anal. Chim. Acta*, 2019, **1092**, 108–116.
23 H. M. Zhao, X. P. Wen, W. Y. Li, Y. Q. Lia and C. X. Yin, *J. Mater. Chem. B*, 2019, **7**, 2169–2176.
24 H. Wu, L. Zhu and V. P. Torchilin, *Biomaterials*, 2013, **34**, 1213–1222.
25 B. B. Zhu, W. Tang, Y. Q. Ren and X. R. Duan, *Anal. Chem.*, 2018, **90**, 13714–13722.
26 Y. Adachi, H. Kawasaki, T. Nagata and Y. Obora, *Chem. Lett.*, 2016, **45**, 1457–1459.
27 Z. B. Gan, Y. J. Lin, L. Luo, G. M. Han, W. Liu, Z. J. Liu, C. H. Yao, L. H. Weng, L. W. Liao, J. S. Chen, X. Liu, Y. Luo, C. M. Wang, S. Q. Wei and Z. K. Wu, *Angew. Chem. Int. Ed*, 2016, **55**, 11567–11571.
28 A. Lavasanifar, J. Samuel and G. S. Kwon, *J. Control. Release*, 2001, **77**, 155–160.
29 M. Abo, Y. Urano, K. Hanaoka, T. Terai, T. Komatsu and T. Nagano, *J. Am. Chem. Soc.*, 2011, **133**, 10629–10637.
30 S. Izumi, Y. Urano, K. Hanaoka, T. Terai and T. Nagano, *J. Am. Chem. Soc.*, 2009, **131**, 10189–10200.
31 H. Zhu, Z. Zhang, S. R. Long, J. J. Du, J. L. Fan and X. J. Peng, *Nat. Protoc.*, 2018, **13**, 2348–2361.
32 H. F. Fang, H. Yu, Q. Lu, X. Fang, Q. L. Zhang, J. T. Zhang, L. L. Zhu and Q. B. Ma, *Anal. Chem.*, 2020, **92**, 12825–12832.
33 L. Z. Hu, L. Deng, S. Alsaiari, D. Y. Zhang and N. M. Khashab, *Anal. Chem.*, 2014, **86**, 4989–4994.
34 J. X. Wang, N. Goswami, T. Shu, L. Su and X. J. Zhang, *Mater. Chem. Front.*, 2018, **2**, 923–928.
35 Y. Yan, S. H. Wang, Z. W. Liu, H. Y. Wang and D. J. Huang, *Anal. Chem.*, 2010, **82**, 9775–9781.

36 C. L. Dantec, J.-P. Duguet, A. Montiel, N. Dumoutier, S. Dubrou and V. Vincent, *Appl. Environ. Microb.*, 2002, **68**, 1025–1032.

37 R. L. Whetten and R. C. Price, *Science*, 2007, **318**, 407–408.

38 J. P. Xie, Y. G. Zheng and J. Y. Ying, *J. Am. Chem. Soc.*, 2009, **131**, 888–889.

39 P. Pyykkö, *Angew. Chem., Int. Ed.*, 2004, **43**, 4412–4456.

40 Y. H. Liu, W. X. Duan, W. Song, J. J. Liu, C. L. Ren, J. Wu, D. Liu and H. L. Chen, *ACS Appl. Mater. Interfaces*, 2017, **9**, 12663–12672.

41 T. Chatzimitakos, A. Kasouni, L. Sygellou, I. Leonardos, A. Troganis and C. Stalikas, *Sens. Actuators, B*, 2018, **267**, 494–501.

42 S. J. Chen, H. Wang, Y. N. Hong and B. Z. Tang, *Mater. Horiz.*, 2016, **3**, 283–293.

43 A. E. Molero, C. C. Altimari, D. A. Duran, E. Garcia, G. Pino-Ramirez and G. E. Maestre, *Clin. Biochem.*, 2006, **39**, 1007–1015.

44 Y. L. Zhang, X. M. Shao, Y. Wang, F. C. Pan, R. X. Kang, F. F. Peng, Z. T. Huang, W. J. Zhang and W. L. Zhao, *Chem. Commun.*, 2015, **51**, 4245–4248.

45 R. Hong, G. Han, J. M. Fernández, B. J. Kim, N. S. Forbes and V. M. Rotello, *J. Am. Chem. Soc.*, 2006, **128**, 1078–1079.

46 A. Karimi, S. Andreescu and D. Andreescu, *ACS Appl. Mater. Interfaces*, 2019, **11**, 24725–24734.

47 E. Laborda, A. Molina, C. Batchelor-McAuley and R. G. Compton, *ChemElectroChem*, 2018, **5**, 410–417.

48 Z. N. Wei, H. Q. Li, S. B. Liu, W. Wang, H. L. Chen, L. H. Xiao, C. L. Ren and X. G. Chen, *Anal. Chem.*, 2019, **91**, 15477–15483.

49 T. Ono, K. Yamashita, T. Murayama and T. Sato, *Biocontrol Sci.*, 2012, **17**, 129–133.

50 J. H. Zhao, J. W. Chen, S. N. Ma, Q. Q. Liu, L. X. Huang, X. N. Chen, K. Y. Lou and W. Wang, *Acta Pharm. Sin. B*, 2018, **8**, 320–338.

51 W. R. Dong, C. M. Sun, M. T. Sun, H. W. Ge, A. M. Asiri, H. M. Marwani, R. Y. Ni and S. H. Wang, *ACS Appl. Nano Mater.*, 2019, **3**, 312–318.

52 T. T. Chen, Y. H. Hu, Y. Cen, X. Chu and Y. Lu, *J. Am. Chem. Soc.*, 2013, **135**, 11595–11602.

53 Q. Zhu, Y. X. Lian, S. Thyagarajan, S. E. Rokita, K. D. Karlin and N. V. Blough, *J. Am. Chem. Soc.*, 2008, **130**, 6304–6305.